

# High-pressure strength and compressibility of titanium diboride (TiB<sub>2</sub>) studied under non-hydrostatic compression

Hao Liang<sup>a,b</sup>, Haihua Chen<sup>a,\*</sup>, Fang Peng<sup>b,\*\*</sup>, Lingxiao Liu<sup>a</sup>, Xin Li<sup>b</sup>, Kui Liu<sup>a</sup>, Chuangqi Liu<sup>c</sup>, Xiaodong Li<sup>d</sup>

<sup>a</sup> Foundation Department of Qinghai University, Xining, 810016, PR China

<sup>b</sup> Institute of Atomic and Molecular Physics, Sichuan University, Chengdu, 610065, PR China

<sup>c</sup> College of Optoelectronic Technology, Chengdu University of Information Technology, Chengdu, 610225, PR China

<sup>d</sup> Institute of High Energy Physics, Chinese Academy of Sciences, Beijing, 100049, PR China

## ARTICLE INFO

### Keywords:

Titanium diboride  
Non-hydrostatic pressure  
Bulk modulus  
Yield strength

## ABSTRACT

The high-pressure strength and plastic properties of titanium diboride (TiB<sub>2</sub>) were investigated using synchrotron angle-dispersive x-ray diffraction (AXRD) under non-hydrostatic compression up to 42 GPa in a diamond-anvil cell (DAC). The AXRD data yielded a bulk modulus  $K_0 = 308 \pm 10$  GPa with a pressure derivative  $K'_0 = 3.4 \pm 1$ . The experimental data are discussed and compared to the results of first-principles calculations. The compressibility of TiB<sub>2</sub> demonstrates a strongly anisotropic property with increasing pressure. In addition, the microscopic deviatoric stress and grain size (crystallite size) were determined as a function of pressure from the line-width analysis. We can see that the strength increases while the crystalline size decreases steeply as the pressure is raised from ambient to about 22 GPa. In other words, TiB<sub>2</sub> starts to yield a plastic deformation at around 22 GPa, and the yield strength of TiB<sub>2</sub> increases with pressure, reaching a value of  $\sim 27$  GPa at the highest pressure in our experiment.

## 1. Introduction

Transition metal diboride ceramics (TiB<sub>2</sub>, CrB<sub>2</sub>, TaB<sub>2</sub>, HfB<sub>2</sub>) are actively investigated because of their useful physical and mechanical characteristics [1]. Titanium diboride (TiB<sub>2</sub>) materials have received wide attention because of their high melting points (about 3000 °C), high hardness (Vickers hardness = 33.7 GPa and Mohs hardness > 9) and elastic modulus, high resistance to corrosion and wear, and fair chemical inertness in metal melts and excellent thermal shock resistance [2,3]. Due to their outstanding properties, they have been extensively used for high-temperature structural materials, cutting tools and hard coating, and have aroused great interest in basic research and several technological applications [4]. It has been reported that TiB<sub>2</sub> has a hexagonal lattice structure ( $C_{32}$ ) of space group no. 191 (P6<sub>3</sub>/mmm), and the lattice parameters were  $a = 3.0292$  Å and  $c = 3.2284$  Å. There are three atoms in the unit cell, all of them in special positions: the Hf atom is on the 1a Wyckoff site (0, 0, 0) and the B atoms are on the 2d Wyckoff site (1/3, 2/3, 1/2) [5]. A hexagonal TiB<sub>2</sub> crystal has six different elastic coefficients ( $C_{11}$ ,  $C_{12}$ ,  $C_{13}$ ,  $C_{33}$ ,  $C_{44}$  and  $C_{66}$ ), but only five of them are independent since  $C_{66} = 1/2 (C_{11} -$

$C_{12})$  [6]. In previous studies [7–15], the bulk modulus of titanium diboride, which ranges from 193 GPa to 399 GPa, has been intensively investigated using experiments and calculations. Several studies have reported on the bonding mechanism, lattice parameters, and elastic properties of TiB<sub>2</sub> using first-principles local-density-functional calculations [16]. Knowledge of the elastic properties, strength, and plastic deformation of TiB<sub>2</sub> ceramic materials is a requisite for understanding its stability and for its applications under extreme static and dynamic mechanical stresses and high temperature. In 2006, TiB<sub>2</sub> was studied by Amulele et al. [17] in a DAC in order to determine its hydrostatic equation of state (EOS) and investigate its strength. The measurements were conducted up to 60 GPa by using the radial x-ray diffraction technique and analyzed using the lattice strain theory [18–20]. Unfortunately, there are relatively few studies devoted to direct experimental measurements on the strength and plastic deformation behavior of titanium diboride by analyzing the x-ray diffraction peak broadening under non-hydrostatic compression.

In this study, the EOS, high-pressure strength and plastic properties of a polycrystalline titanium diboride sample were investigated using a diamond anvil cell (DAC) by synchrotron angle-dispersive x-ray

\* Corresponding author. Foundation Department of Qinghai University, Xining, 810016, PR China.

\*\* Corresponding author. Institute of Atomic and Molecular Physics, Sichuan University, Chengdu, 610065, PR China.

E-mail addresses: [chenghaihua06@163.com](mailto:chenghaihua06@163.com) (H. Chen), [fangpeng18@yahoo.com](mailto:fangpeng18@yahoo.com) (F. Peng).

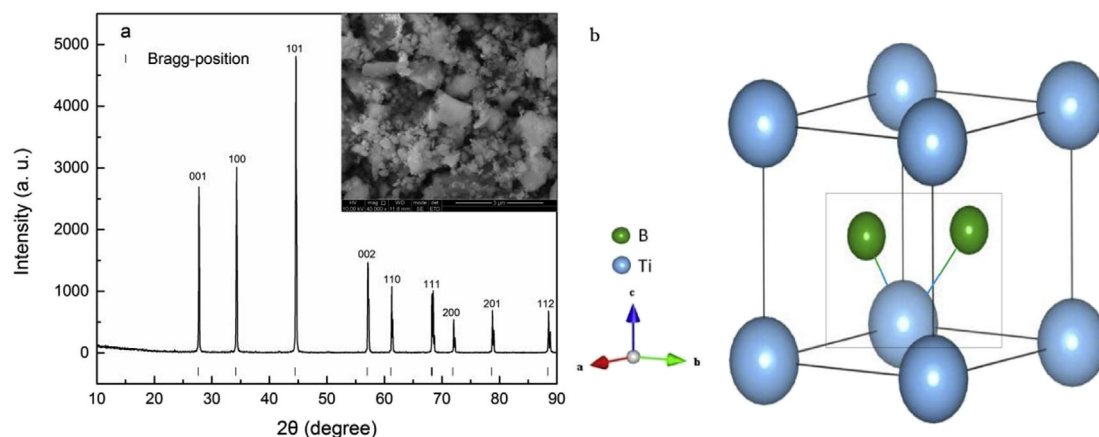


**Fig. 1.** (a) X-ray diffraction patterns ( $\lambda = 1.5404 \text{ \AA}$ ) of the initial powder under normal pressure and room temperature. Upper-right inset: scanning electron microscope (SEM) images of starting powder. (b) Schematic crystal structures of  $\text{TiB}_2$ .

diffraction (AXRD) under uniaxial compression up to 42 GPa. For comparison with previous and experimental results, the elastic properties of  $\text{TiB}_2$  were calculated using first-principles density functional theory (DFT).

## 2. Material and methods

### 2.1. Experimental procedures

Polycrystalline titanium diboride powder (99.99% purity, 0.5–1  $\mu\text{m}$  grain size) was purchased from the Alfa Aesar Co., Ltd., Shanghai China. The initial powder was characterized by x-ray diffraction (XRD; model DX-2500, Dandong, China) using a  $\text{Cu K}\alpha$  radiation source with  $\lambda = 1.5404 \text{ \AA}$  to check the crystal structure, purity and morphology. Fig. 1a shows the power XRD pattern and scanning electron microscope (SEM) images of the starting specimen. As shown in Fig. 1b,  $\text{TiB}_2$  has a hexagonal structure. An in situ high pressure AXRD experiment was carried out using a symmetric-type DAC with a culet size of 300  $\mu\text{m}$ , which was interfaced with angle-dispersive synchrotron radiation at the 4W2 beamline of the Beijing Synchrotron Radiation Facility (BSRF, China) at room temperature.  $\text{TiB}_2$  powders were loaded into an 80- $\mu\text{m}$ -diameter hole of a stainless steel T301 gasket that was pre-indented to  $\sim 30 \mu\text{m}$  thickness at  $\sim 18 \text{ GPa}$ . With the ruby fluorescence method, the pressure was determined during such an experiment. No pressure-transmitting medium was used to achieve a maximum non-hydrostatic pressure environment. In situ diffraction patterns of the sample were recorded using a two-dimensional imaging plate detector (MAR-3450) for further analysis. The Bragg diffraction rings were converted into a series of one-dimensional intensity versus diffraction angle  $2\theta$  patterns using the FIT2D program. It allows for detector calibration and integration of powder diffraction data from 2D detectors to 1D  $2\theta$  scans using a  $\text{CeO}_2$  calibration material from NIST. The Rietveld refinements of powder x-ray diffraction data were carried out using the General Structure Analysis System (GSAS) program as implemented in the EXPGUI package.

### 2.2. Theoretical calculations

In this study, the ab initio simulations based on DFT calculations were performed using the ultrasoft pseudo-potentials plane wave technique, the Cambridge Serial Total Energy Package (CASTEP) code [21]. The exchange-correlation function is described in generalized gradient approximation (GGA) [22]. The elastic modulus and phase stability of  $\text{TiB}_2$  were obtained by using DFT. Ultrasoft pseudo-potentials were used to characterize the interactions between electrons and the ionic core. The plane wave cut-off energy was chosen as 560 eV, and

$9 \times 9 \times 2$  Monkhorst-Pack k-point sampling was used for all cases. The tolerances for geometry optimization were set as the difference of total energy within  $5 \times 10^{-6} \text{ eV/atom}$ , maximum ionic Hellmann-Feynman force within  $0.01 \text{ eV/\AA}$ , maximum ionic displacement within  $5 \times 10^{-4} \text{ \AA}$ , and maximum stress within 0.02 GPa.

Convergence tests revealed that the parameters described above were sufficient to lead to a well-converged total energy, which are carefully tested in the text. The bulk modulus at ambient pressure ( $K_0$ ) and its pressure derivative ( $K'_0$ ) were determined by fitting the numerical data to the isothermal Birch-Murnaghan EOS.

### 2.3. Line-width analysis

A polycrystalline sample compressed with non-hydrostatic uniaxial compression in a DAC produces complex stresses and resulting strains in the sample. These stresses can be thought of as a superposition of two types of stresses, macro-differential stress (macro-DS)  $t$  and micro-deviatoric stress (micro-DS)  $\epsilon$  [23]. There were two different methods for strength of materials under large non-hydrostatic compression: analysis of x-ray diffraction peak broadening and measurement of peak shifts associated with lattice strains. He et al. [24] have reported on the consistency of the two approaches.

The diffraction line broadening under non-hydrostatic compression is attributed to two different factors: the reduction in grain size and the presence of micro-strains. The theory proposed earlier for diffraction line broadening from deformed metals was extended for the analysis of high pressure data [25]. The following relation describes the grain size and strain dependencies of diffraction line widths [26]:

$$(2\omega_{hkl} \cos \theta_{hkl})^2 = (\lambda/d)^2 + \eta_{hkl}^2 \sin^2 \theta_{hkl}, \quad (1)$$

where  $2\omega_{hkl}$  denotes the full width at half-maximum (FWHM),  $\theta_{hkl}$  is the Bragg angle,  $\lambda$  is the wavelength of the x-ray, and  $d$  is the grain size of the crystallites. Meanwhile,  $\eta_{hkl}$  denotes the microscopic deviatoric strain and depends on Young's modulus  $E$ .

Once plastic deformation is initiated, macro-DS  $t$  and micro-DS  $\epsilon$  that the aggregate polycrystalline sample can support are equal to the yield strength  $Y$ . The relationship is as follows:

$$Y = t = \epsilon E, \quad (2)$$

where  $\epsilon$  is the average value of  $\eta_{hkl}$ . The aggregate  $E$  can be obtained from the bulk modulus  $K$  and shear modulus  $G$  using [26]:

$$E = 9KG/(3K + G) \quad (3)$$

## 3. Results and discussion

The AXRD patterns of  $\text{TiB}_2$  under high pressure up to 42 GPa are

Download English Version:

<https://daneshyari.com/en/article/7919968>

Download Persian Version:

<https://daneshyari.com/article/7919968>

[Daneshyari.com](https://daneshyari.com)